ACS APPLIED MATERIALS & INTERFACES

Research Article

www.acsami.org

Novel Polymer Gel Electrolyte with Organic Solvents for Quasi-Solid-State Dye-Sensitized Solar Cells

Sheng-Yen Shen,[†] Rui-Xuan Dong,[†] Po-Ta Shih,[†] Vittal Ramamurthy,[‡] Jiang-Jen Lin,*[,†] and Kuo-Chuan Ho*[,†,‡]

[†]Institute of Polymer Science and Engineering, National Taiwan University, Taipei 10617, Taiwan

[‡]Department of Chemical Engineering, National Taiwan University, Taipei 10617, Taiwan

Supporting Information

ABSTRACT: A cross-linked copolymer was previously synthesized from poly(oxyethylene) diamine (POE-amine) and an aromatic anhydride and cured to generate an amide-imide cross-linking structure. The copolymer containing several chemical groups such as POE, amido acids, and imide, enabled to absorb liquid electrolytes in methoxypropionitrile (MPN) for suitable uses in dye-sensitized solar cells. To establish the advantages of polymer gel electrolytes (PGE), the same copolymer was studied by using different electrolyte solvents including propylene carbonate (PC), dimethylformamide, and *N*-methyl-2-pyrrolidone, and shown their long-term stability. The morphology of the copolymer after absorbing liquid electrolytes in these solvents was proven the same as a 3D interconnected nanochannels, evidenced field emission-scanning electron microscopy. Among these solvents, PC was selected as the optimized PGE, which demostrated a higher power conversion efficiency (8.31%) than that of the liquid electrolyte (7.89%). In particular, the long-term stability of only a 5% decrease in the cell efficiency after 1000 h of testing was achieved. It was proven the developed copolymer as PGE was versatile for different solvents showing high efficiency and long-term durability.

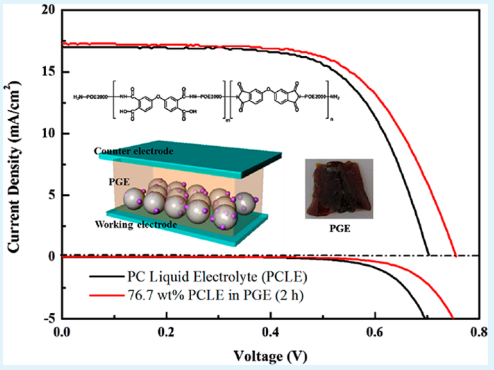

KEYWORDS: *cross-linked polymer, elastomeric structure, polymer gel electrolyte, matrix for electrolytes, quasi-solid-state dye-sensitized solar cell, solvents*

INTRODUCTION

Dye-sensitized solar cells (DSSCs) have received attention due to their attractive features, such as high energy conversion efficiency, possible low cost of production, and environment friendly nature; these advantages make them attractive to substitute conventional silicone photovoltaics as a new solar energy source.[1,2] However, as we know, the traditional DSSCs based on organic liquid electrolytes still have some problems to be solved. For example, the sealing issue of the cells, the dissociation of the dye absorbed on TiO_2, and the volatility of organic solvent, which caused poor long-term stability at high temperatures.[3−5] Hence, many efforts have been made to replace liquid electrolytes with ionic liquids,[6,7] organic hole transport materials,[8] *p*-type inorganic semiconductors,[9,10] polymers,[11] and quasi-solid-state gel-electrolytes for DSSCs.[12−14] Several polymer or copolymer materials have been proposed to prepare polymer gel ionic liquid electrolytes for DSSCs.[15,16] However, the quasi-solid-state dye-sensitized solar cell (QSS-DSSC) exhibited lower power conversion efficiency (η) compared to the liquid electrolyte solar cell. This is attributed to the high electron-transfer resistance at the electrolyte/counter electrode interface and the high viscosity of gel electrolyte, which cannot easily penetrate into the pores of the TiO_2 film of the solar cell. Therefore, the above items are the major concerns of quasi-solid electrolytes of DSSCs.

Polymer gel electrolytes (PGEs), a polymer matrix absorbed with liquid electrolyte, belong to a potential alternative to solid-state electrolytes for the fabrication of DSSCs. PGEs contain several advantages such as the enhancement of ionic conductivity, and the well interfacial filling property to penetrate into the TiO_2 photoelectrode.[17,18] Also, it shows good long-term stability compared to liquid electrolyte of DSSC due to the reduced leakage of solvent. The formation of PGE generally involves a 3D network structure in which liquid electrolyte is absorbed in the cages. According to the literature, the polymers for preparing PGEs were reported to be poly(acrylonitrile),[19] poly(methyl acrylate) (PMA),[20] poly(vinylidene fluoride-*co*-hexafluoropropylene) (PVDF-HFP),[21] poly(methyl methacrylate) (PMMA),[22] and poly(acrylic acid) (PAA).[8] The polymer containing poly(ethylene glycol) (PEG) or poly(oxytheylene) (POE) segment was also used for its ability of absorbing polar liquid electrolytes and its high chemical stability.[23] Further, the POE structure,

Received: January 5, 2014
Accepted: October 9, 2014
Published: October 9, 2014

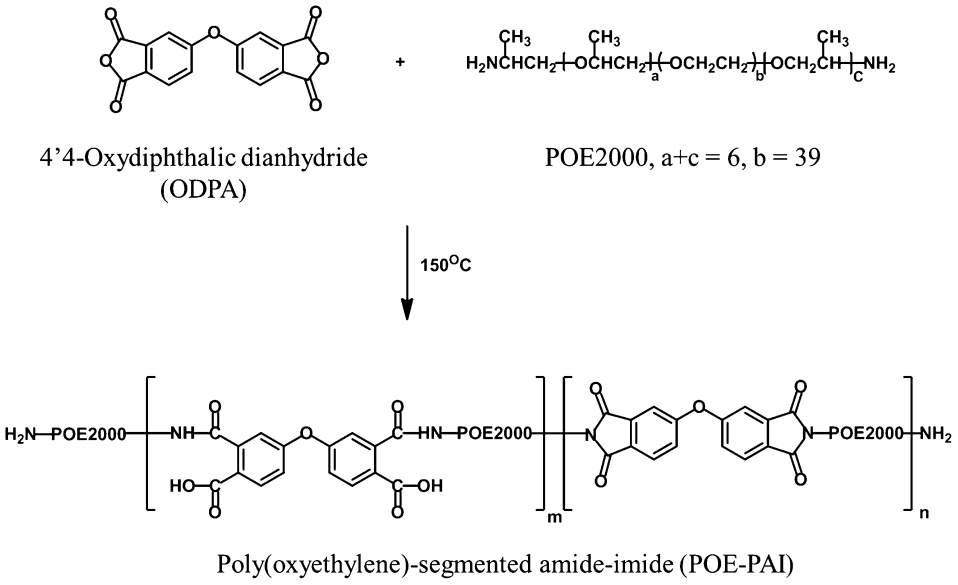

Figure 1. Scheme for the preparation of poly(oxyethylene)-segmented amide−imide (POE-PAI).

$-(CH_2CH_2O)_x-$, could interact well with TiO_2 through the noncovalent bonding force and reduce the pertinent recombination from TiO_2 to I_3^- at the interface of TiO_2/electrolyte.[24] Another polymer, PVDF-HFP, for PGEs was found to render high stabilities and high conversion efficiencies for DSSCs, when sensitized with hydrophobic ruthenium dyes.[21,25] In general, these PGEs were found to be less efficient than the conventional liquid electrolytes in terms of power conversion efficiencies in DSSCs.[26,27]

Previously, we have developed a novel structure of POE containing amide−imide copolymer (POE-PAI)[13] and used it to absorb liquid electrolytes for QSS-DSSC. In the previous work, we used the liquid electrolyte containing LiI/I_2 and methoxypropionitrile (MPN) solvent but lacking the knowledge of its suitability for different electrolytes or solvents and its problem of long-term stability. In this work, we studied the cross-linked copolymer POE-PAI for its capability of absorbing various liquid electrolytes prepared with different solvents, including propylene carbonate (PC), dimethylformamide (DMF), and *N*-methyl-2-pyrrolidone (NMP). We further confirmed their morphologies by showing well-defined nanochannels, thus the changes in power conversion efficiency of DSSC. More importantly, the most suitable solvent, PC, was selected for fabricating the DSSC to demonstrate a long-term durability of 1000 h under the standard test.

EXPERIMENTAL SECTION

Materials. POE-amine with a molecular weight of 2000 g × mol^{-1}, and structure of 6 oxypropylene and 39 oxyethylene units, was obtained from Huntsman Chemical Co. Monomer 4,4′-oxydiphthalic anhydride (ODPA, 97% purified by sublimation), titanium(IV) isopropoxide (TTIP, 98%), 4-*tert*-butylpyridine (TBP, 96%), and *t*-butanol (TBA, 99.5%) were obtained from Aldrich Chemical Co. *cis*-Bis(isothiocyanato)bis(2,2′-bipyridyl-4,4′-dicarboxylato) ruthenium-(II)-bis-tetrabutylammonium (N719), 1,2-dimethyl-3-propylimidazolium iodide (DMPII), ionomer resin (Surlyn, SX1170-25, thickness = 25 μm), fluorine-doped SnO_2 glass (FTO, surface resistivity = 15 Ω sq^{-1}) were obtained by Solaronix S. A. Anhydrous LiI, I_2, and acetonitrile (ACN) were bought from Merck Chemical Co. The solvents, propylene carbonate (PC), dimethylformamide (DMF), and *N*-methyl-2-pyrrolidone (NMP), were procured from Fluka. Tetrahydrofuran (THF, 95%) received from Teida Chemicals. The dispersant of TiO_2, POE segmented imide (POEM) was synthesized in our laboratory.

Synthesis of the POE−Amide−Imide Copolymers. Amphiphilic polymer gel was synthesized as the procedures from ref 13: POE2000 (30.0 g, 0.015 mol) was added and dissolved in 20 mL of THF. Subsequently, ODPA (3.1 g, 0.01 mol) dissolved in 10 mL of THF and then poured into the solution. Under nitrogen atmosphere, the polymerization reaction temperature was maintained at 150 °C under vigorous stirring for 3 h. Then, the mixture became viscous with its color changed from yellow to yellow-brown. Finally, the product was kept in the oven at 80 °C for several days to allow the conversion into an elastomeric solid (Figure 1).

Preparation of the PGEs. The polymer gel electrolyte was prepared by soaking in liquid electrolyte for different times. The component of liquid electrolyte is 0.6 M DMPII, 0.1 M LiI, 0.05 M I_2, and 0.5 M TBP in PC, NMP, or DMF. The polymer was a coil, and in its coil form, it could fully or partially enter the TiO_2 film; its soft, sticky, and elastic nature also enables it to penetrate well into the pores of the TiO_2 film. To verify this, we have obtained cross sectional scanning electron microscopy (SEM) images of bare TiO_2 film, bare PGE film, and TiO_2 film with PEG. The cross sectional FE-SEM images of the DSSCs with (a) TiO_2/FTO layer, (b) PGE/TiO_2/FTO layer, (c) PGE/TiO_2/FTO layer (large scale), and (d) PGE are shown in Figure S1 of the Supporting Information. Figure S1 (Supporting Information) clearly demonstrates the incorporation of the PGE in the TiO_2 film. The PGE in Figure S1d (Supporting Information) has a nanochannel structure.

Fabrication of the DSSC. The nanoporous TiO_2 photoanode was performed through the following procedures: The FTO glass was cleaned by four steps: neutral cleaner, water, acetone, and IPA. Then, a solution consisting of TTIP and 2-methoxyethanol using spin-coating coated on the FTO glass to form a compact layer. This layer serves as a good mechanical contact between the FTO and the TiO_2 and also as an insulator between the FTO and the electrolyte. The TiO_2 nanoparticle was synthesized by sol−gel method and a hydrothermal process from the literature.[13] The concentration of TiO_2 colloid was adjusted to 13 wt %. Then, 30 wt % of POEM was added to prevent the TiO_2 aggregation and control the pore size of TiO_2 paste. Subsequently, the homogeneous TiO_2 paste was coated on the FTO glass using doctor blade technique to obtain a TiO_2 film. The TiO_2 film was sintered at 450 °C for 30 min, then repeated coating and sintering for more time. The anatase TiO_2 film of 16 μm in thickness was obtained. Finally, the TiO_2 photoanode was completed by immersing the TiO_2 film in 0.3 mM N719 (solution) at room temperature for 24 h.

The DSSC was fabricated by sandwiching a polymer gel electrolyte between the TiO_2 photoanode and a platinum (Pt) counter electrode. The thickness of PGE is controlled using Surlyn (25 μm thick), which also acts as a spacer between the photoanode and counter electrode.

Instruments and Analyses. The surface morphologies of PGE and cross sectional morphologies of the quasi-solid-state DSSC were observed using field emission scanning electronic microscopy (FE-SEM, Zeiss EM 902A). The current−voltage (I−V) curve was measured using a class A quality solar simulator (PEC-L11, AM1.5, 100 mW/cm^2, Peccell Technologies, Inc.). The light intensity (100 mW/cm^2) was calibrated with a standard Si cell (PECSI01, Peccell Technologies, Inc., Kanagawa, Japan). Electrochemical impedance spectroscopy (EIS) was recorded with a potentiostat (PGSTAT 30, Autolab, Eco-Chemie, The Netherlands) under an illumination of 100 mW/cm^2. The frequency range was varied from 10 mHz to 65 kHz, and the magnitude of the alternating signal was 10 mV. For measuring the ionic conductivity of an electrolyte, a symmetric cell was used, in which the electrolyte was sandwiched between two Pt coated FTO electrodes, using a 25 mm thick Surlyn film as the spacer. The incident photo-to-current conversion efficiency (IPCE) curve was measured as a function of wavelength from 400 to 800 nm.

RESULTS AND DISCUSSION

Absorption Behavior of the Polymer Gel for Liquid Electrolytes with Different Solvents. The copolymer or polymer gel consists of POE segments, aromatic imide functionalities, and carboxylic acids, as presented in Figure 1. The scheme shows the synthetic route of this polymer gel. The carboxylic acids of ODPA react with the terminal amines of POE−amine to obtain the cross-linked structure, i.e., POE-PAI, which is an elastomer. The gel-like copolymer was allowed to absorb a liquid electrolyte to prepare the polymer gel electrolyte for a DSSC. The liquid electrolyte contained 0.6 M DMPII, 0.5 M TBP, 0.1 M LiI, 0.05 M I_2 in an organic solvent, precisely, DMF, PC, or NMP. Figure 2 shows absorption behavior of the copolymer for liquid electrolytes with various solvents for different periods of its soaking in the liquid electrolytes (the absorption is shown in terms of wt % of the absorbed liquid electrolyte). Figure 2 shows that all the three liquid electrolytes are absorbed by at least 63% of their initial weight at the end of 30 min, then up to 81 wt % of their initial weight after 3 h. Interconnected channels and POE segments of the PGE are believed to have facilitated the absorption of the liquid electrolytes. The absorption of the liquid electrolyte prepared with the PC liquid electrolyte is the slowest among all, because of the higher viscosity of PC, compared to those of DMF and NMP. This is the reason for the faster swelling of the copolymer in NMP and DMF, compared to that in PC. The swelling of the copolymer in DMF is better than that in NMP; this is also the reason for higher viscosity of NMP than that of DMF. The insets in Figure 2 show digital photographs of the POE-PAI copolymer, before and after its soaking for 3 h in the PC liquid electrolyte.

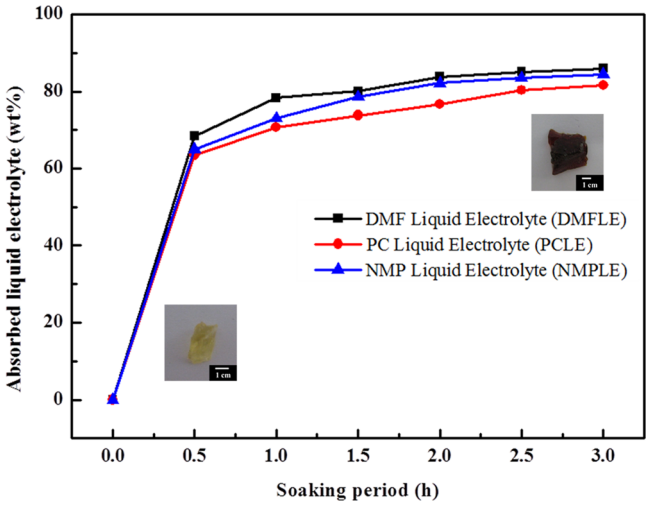

Figure 2. Absorption behavior of the copolymer for liquid electrolytes with different solvents for different periods of its soaking in the liquid electrolytes (the absorption is shown in terms of wt % of the absorbed liquid electrolyte). The insets show digital photographs of the POE-PAI copolymer, before its soaking in the PC liquid electrolyte (lower one) and after its soaking in the PC liquid electrolyte (upper one).

The FE-SEM images of polymer gel electrolyte were employed for observing the surface morphologies as shown in Figure 3. Figure 3a,c shows micrographs of POE-PAI before soaking in the PC liquid electrolyte, and Figure 3b,d shows those of the same material after soaking in the PC liquid electrolyte. The morphology of POE-PAI without the electrolyte is formless and its surface is smooth, as shown in Figure 3a,c. However, after the absorption of the PC liquid electrolyte, approximately 200−500 nm nanochannels have been observed (Figure 3b,d). According to this result, it can demonstrate that the elastomer has 3D interconnected nanochannels after the absorption of the PC liquid electrolyte and caused the elastomer to swell. The microstructure of the swollen elastomer was dimensionally stable when it absorbed PC liquid electrolyte within 24 h.

Photovoltaic Performance of the DSSCs Using the Polymer Gel Electrolyte with Different Solvents. Table 1 shows the photovoltaic parameters of the DSSCs with the same PGE electrolyte containing different solvents. The table also shows the photovoltaic parameters of the DSSCs with bare liquid electrolytes (without PGE) prepared with these solvents. The table shows that the DSSC using the PGE with the PC liquid electrolyte exhibits a higher V_{OC}, J_{SC}, and power conversion efficiency (η) than those of its corresponding DSSC with the bare PC liquid electrolyte, i.e., the PC liquid electrolyte without the copolymer. It is also clear from Table 1 that the DSSC containing PGE with PC shows the best performance among all the DSSCs. The table also gives the physical properties of the solvents, i.e., the boiling point, donor number, viscosity, and dielectric constant. Table 1 shows no specific correlation between boiling point and photovoltaic parameters or between viscosity and photovoltaic parameters. With increases in dielectric constant, the conductivity increases, the J_{SC} increases, and consequently, the power conversion efficiency of the pertinent DSSC increases. A high dielectric solvent in a polymer electrolyte can increase the polarity in the electrolyte, and thereby can decrease ion−ion interactions in the electrolyte, and thus ultimately can increase the ionic mobility in the electrolyte. In regards to donor number, the J_{SC} (and thereby η) will be lower for a DSSC, if the donor number of the solvent for its electrolyte is higher. Kebede and Lindquist have studied donor−acceptor reactions between iodine and nonaqueous solvents.[28] It is disclosed that the donor number of a solvent can control the equilibrium of iodide and triiodide ions in the solvent. The increase of the donor number in the solvent will decrease the concentration of the free I_3^- and increase the concentration of the free I^-, which promotes the improvement of the hole collection.[29] The complex of solvent and iodine can be much more easily formed when a solvent with higher donor number is used in a DSSC, which increases

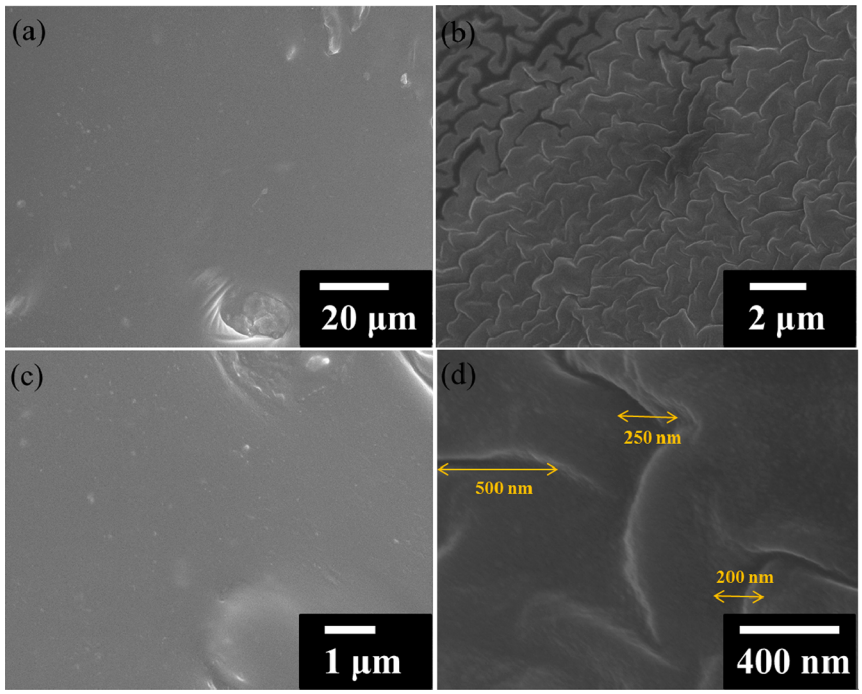

Figure 3. FE-SEM images of the POE-PAI copolymer, before (a,c) and after (b,d) its soaking in the PC liquid electrolyte.

Table 1. Physical Properties of the Organic Solvents Used in This Study, And Photovoltaic Parameters of the DSSCs with the Same PGE Containing These Solvents[a]

DSSC electrolyte	bp (°C)	DN[b]	viscosity (cp)	ε_r[c]	σ (mS/cm)	polymer conc. (wt %)	V_{OC} (V)	J_{SC} (mA/cm^2)	FF	η (%)
PGE with DMF	153	26.6	0.92	36	9.81 ± 0.14	20.4 ± 0.97	0.73 ± 0.01	12.70 ± 0.05	0.73 ± 0.01	6.77 ± 0.04
liquid electrolyte with DMF					9.67 ± 0.06	0	0.72 ± 0.01	11.85 ± 0.09	0.71 ± 0.01	6.06 ± 0.07
PGE with PC	242	15.1	2.52	65	10.96 ± 0.12	23.3 ± 0.66	0.76 ± 0.01	17.35 ± 0.06	0.63 ± 0.01	8.31 ± 0.04
liquid electrolyte with PC					10.92 ± 0.05	0	0.70 ± 0.01	17.07 ± 0.12	0.66 ± 0.01	7.89 ± 0.09
PGE with NMP	204	27.3	1.65	32.2	7.88 ± 0.11	25.0 ± 0.76	0.76 ± 0.01	11.98 ± 0.06	0.63 ± 0.01	5.74 ± 0.06
liquid electrolyte with NMP					7.73 ± 0.05	0	0.71 ± 0.01	11.19 ± 0.14	0.59 ± 0.01	4.69 ± 0.10

[a]Photovoltaic parameters are also shown for the DSSCs with bare liquid electrolytes (without PGE) prepared with these solvents. [b]Donor number. [c]Dielectric constant.

the V_{OC} of the DSSC. A solvent with a higher donor number shows a higher Lewis basicity and reacts in an easier way with the corresponding Lewis acidic TiO_2; this enables more efficient blocking of active sites of TiO_2, thereby decreasing the recombination rate of I_3^- ions with the injected electrons and increasing the V_{OC} of the pertinent DSSC.[30] The DSSC with PC exhibits the best performance, because of the highest conductivity and the lowest donor number of PC, compared to those of DMF and NMP.[31] The DSSC with NMP shows the poorest performance, because of its lowest conductivity and highest donor number, compared to those of PC and DMF. Thus, PC solvent was used to prepare the liquid electrolyte in further studies.

Effect of Concentration of I^-/I_3^- Redox Couple in the Polymer Gel Electrolyte on the Ionic Conductivity of the Electrolyte. It is known that the power conversion efficiency of a DSSC dependents greatly on the ionic conductivity of its electrolyte, which, in turn, should depend on the concentration of I^-/I_3^- redox couple (here LiI + I_2) in the electrolyte. Figure 4 shows the effect of concentration of I^-/I_3^- redox couple in the polymer gel electrolyte with PC on the ionic conductivity of the electrolyte. It can be seen that the conductivity increases steeply with the concentration increase and reaches a maximum value of 10.9 mS/cm with 0.1 M LiI and 0.05 M I_2; the conductivity thereafter decreases steadily. The initial increase in the conductivity of the PGE is probably due a chelation of lithium-metal ions by POE segments of the PGE. This chelation of Li^+ ions favors the transport of I_3^- and I^- ions in the electrolyte. The subsequent decrease in the conductivity of the PGE is apparently due to a great increase in the viscosity of the PGE due to an excessive addition of the salt of LiI.

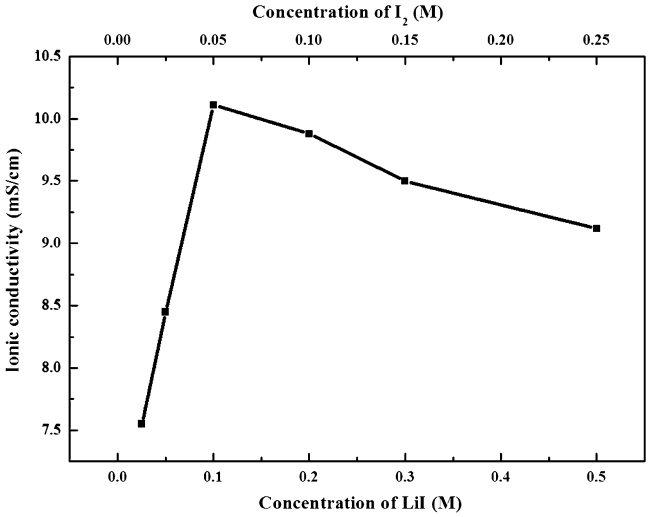

Figure 4. Effect of concentration of the redox couple (LiI + I_2) on the conductivity of the PGE with PC (molar ratio of LiI to I_2 = 2:1).

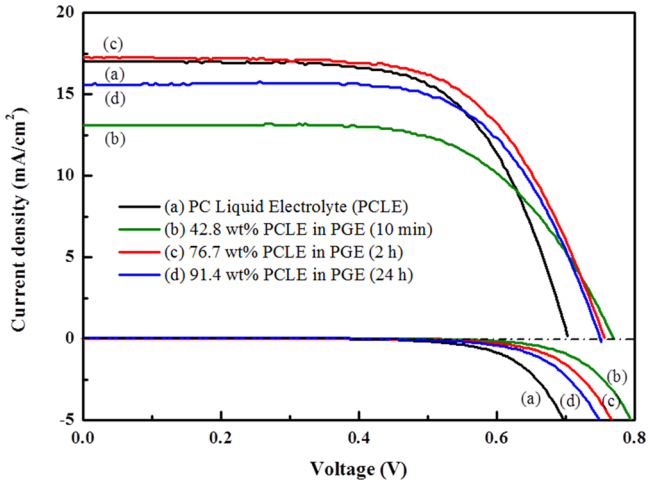

Figure 5. Photocurrent density–voltage curves of the DSSCs with pure PC liquid electrolyte (PCLE) and different concentrations of PCLE in their PGEs, (a) PC liquid electrolyte, (b) 42.8 wt % PCLE in PGE, (c) 76.7 wt % PCLE in PGE, and (d) 91.4 wt % PCLE in PGE, measured at 100 mW cm^{-2}.

Photovoltaic Performance of the DSSCs Using the Polymer Gel Electrolyte with Various Concentrations (wt %) of the PC Liquid Electrolyte. Table 2 shows the elastomer absorption of the PC liquid electrolyte in varing weight ratios for different periods of time (see also Figure 2). In the first row of the table, with the absence of the PGE, the electrolyte of the pertinent DSSC is assumed to be 100% liquid. Table 2 also shows the ionic conductivities of the PGEs prepared with the PC liquid electrolyte at different stages of its absorption. Additionally, the table shows the photovoltaic parameters of the DSSCs using these PGEs. Figure 5 shows the photocurrent density–voltage (J–V) curves corresponding to Table 2; however, for selective DSSC, the figure also shows the corresponding dark current density–voltage curves. The J–V curves of the reference cell (without the PGE, see Table 2) are also shown in Figure 5. The DSSC with the PGE with 76.7% of the PC liquid electrolyte (correspoinding to 2 h in Table 2) shows the highest η of 8.31%. The power conversion efficiency in QSS-DSSC is higher than that of liquid-state DSSC. At the same time, it avoids the disadvantages of liquid-state DSSC. This marks an important improvement for QSS-DSSC. It can be seen in Table 2 that the values of V_{OC} of the cells with PGE are all higher than those with bare PC liquid electrolyte. The increases in the V_{OC} for the cells with PGE can be attributed to the fact that the polymer can penetrate into the TiO_2 films to suppress the recombination reactions. The dark currents in Figure 5 clearly show that the PGE can suppress the recombination reactions effectively. The slightly higher J_{SC} value of the DSSC with 76.7 wt % of the liquid electrolyte, compared to that of the cell with bare PC liquid electrolyte will be explained at a later stage by means of electrochemical impedance spectra (EIS). The DSSC with 42.8 wt % of the PC liquid electrolyte (10 min) is expected to have insufficient amount of I^- and I_3^- ions, which results in a poor charge transport in the electrolyte and thereby in a poor J_{SC} and power conversion efficiency to the pertinent DSSC (Table 2). With the increase of the soaking time to 2 h (76.7 wt % of the PC liquid electrolyte), the amount of I^- and I_3^- ions increases, which, in turn, increases the charge transport in the electrolyte and consequently the J_{SC} and power conversion efficiency of the pertinent DSSC, compared to those of the DSSC with 42.8 wt % of the PC liquid electrolyte. With further increases in the concentration of the PC liquid electrolyte (91.4%), the J_{SC} and power conversion efficiency of the cell decreases, compared to those of the cell with 76.7 wt % of the PC liquid electrolyte; this point will be taken up in the EIS discussion below.

Figure 6 presents Nyquist plots of the DSSCs using the PGEs prepared with the PC liquid electrolyte at different stages of its absorption; the equivalent circuit is shown as an inset in the figure. Generally, the EIS spectra have three semicircles in a DSSC. The corresponding three resistances are related to the electrochemical reaction at the electrolyte/Pt counter electrode (R_{ct1}), the charge-transfer resistance at the TiO_2/dye/electro-

Table 2. Percentage of Absorption of the PC Liquid Electrolyte by the Copolymer for Different Periods of Time, Conductivities of the PGEs Prepared with the PC Liquid Electrolytes at These Periods, And Photovoltaic Parameters of the DSSCs Using These PGEs[a]

period of time	wt %[b]	σ (mS/cm)	J_{SC} (mA/cm^2)	V_{OC} (V)	FF	η (%)
PC liquid electrolyte (PCLE)	100.0	10.92 ± 0.05	17.07 ± 0.12	0.70 ± 0.01	0.66 ± 0.01	7.89 ± 0.09
10 min	42.8 ± 0.18	8.59 ± 0.07	13.09 ± 0.11	0.77 ± 0.01	0.63 ± 0.01	6.35 ± 0.08
30 min	63.5 ± 0.21	10.05 ± 0.05	14.13 ± 0.09	0.76 ± 0.01	0.66 ± 0.01	7.09 ± 0.07
1 h	70.7 ± 0.38	10.04 ± 0.08	14.52 ± 0.15	0.75 ± 0.01	0.67 ± 0.01	7.30 ± 0.12
2 h	76.7 ± 0.66	10.96 ± 0.12	17.35 ± 0.06	0.76 ± 0.01	0.63 ± 0.01	8.31 ± 0.04
6 h	85.7 ± 1.12	10.16 ± 0.18	14.46 ± 0.08	0.77 ± 0.01	0.65 ± 0.01	7.24 ± 0.06
24 h	91.4 ± 1.25	10.17 ± 0.19	14.67 ± 0.11	0.76 ± 0.01	0.65 ± 0.01	7.25 ± 0.09

[a]Photovoltaic parameters at 100 mW cm^{-2}; each value is an average of four measurements. [b]wt %: weight percentage of the PC liquid electrolyte.

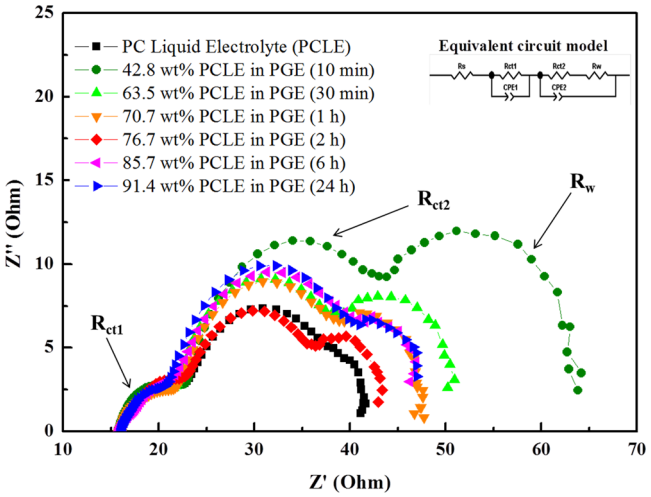

Figure 6. Nyquist plots of the DSSCs with various amounts of PC liquid electrolyte in their PGEs, obtained at AM 1.5 (100 mW cm^{-2}); the equivalent circuit is shown as the inset.

lyte (R_{ct2}), and the Warburg diffusion process (R_w) of I^-/I_3^- in the electrolyte. By carefully examining Figure 6, Table 3, and

Table 3. Electrochemical Impedance Parameters of the Dye-Sensitized Solar Cells with Pure PC Liquid Electrolyte and with PGEs Having Different Concentrations of the PC Liquid Electrolyte, Measured at 100 mW cm^{-2} [a]

electrolyte	wt %[b]	R_{ct1} (Ω)	R_{ct2} (Ω)	R_w (Ω)
PC liquid electrolyte (PCLE)	100.0	10.13	21.62	14.08
10 min	42.8	17.72	26.58	34.64
30 min	63.5	12.41	23.3	16.82
1 h	70.7	12.25	23.6	15.23
2 h	76.7	9.54	19.71	13.03
6 h	85.7	12.53	26.17	15.78
24 h	91.4	12.77	26.08	16.68

[a]These resistance values were evaluated from Figure 6. [b]wt %: wt % of the liquid electrolyte.

Table 2, it can be said that the J_{SC} values of the cells in Table 2 are, in general, qualitatively consistent with the R_{ct1} and R_{ct2} values of these cells in Table 3. Two factors that limit the short-circuit photocurrent (J_{SC}), among others, are the efficiency of collecting the injected electrons at the transparent back contact and the catalytic ability of the counter electrode for the reduction of I_3^- ions to I^- ions. If R_{ct2} is high, the efficiency of collecting the injected electrons at the transparent back contact increases, which in turn increases the rate of electron transfer in the circuit, and thereby the short-circuit photocurrent (J_{SC}) of the pertinent DSSC. If R_{ct1} is high, the rate of reduction of I_3^- ions and creation of I^- ions increases, which in turn increases the rate of regeneration of oxidized dye, the injection of electrons from the regenerated dye, and thereby the J_{SC}. As expected, the value of R_w changed with the composition of the PGE. Figure 5 clearly shows this variation. The R_w values are in consistency with the J_{SC} values of the corresponding DSSCs. The DSSC with 76.7 wt % of the PC liquid electrolyte shows the least R_{ct1} and R_{ct2} values (Table 3), and highest J_{SC} and η values (Table 2). The conductivity of the gel electrolyte with 76.7 wt % of the PC is the highest among the conductivities of other gel electrolytes (Table 2); therefore, the diffusion rate of $I^-$and I_3^- ions in this gel electrolyte could be the highest among all the diffusion rates of these ions in their respective electrolytes; this has apparently led to the highest J_{SC} and η values of the DSSC with this gel electrolyte (Table 2). The R_w value of the DSSC with bare PC liquid electrolyte is, however, smaller than that of the DSSC using PGE with 76.7 wt % of the PC liquid electrolyte; this is consistent with their FF values. Careful observation indicates that the R_{ct1} and R_{ct2} values of the DSSC using PGE with 76.7 wt % of the PC liquid electrolyte are slightly lesser than those of the DSSC using bare PC liquid electrolyte; this may be the reason for the better J_{SC} in favor of the former cell (17.3 mA/cm^2), compared to that of the later cell (17.1 mA/cm^2).

In Figure S2 (Supporting Information), the IPCE of PGE containing 76.7 wt % of the liquid electrolyte was drawn as a function of excitation wavelength and exhibited a plateau at 89%. By comparison, a maximum of 85% for the cell with pure liquid electrolyte was reached. These results are consistent with the J_{SC} values to explain why the J_{SC} value of PGE containing 76.7 wt % of the liquid electrolyte is slightly higher than that of PC liquid electrolyte (Table 2).

Long-Term Stability. As expected, the best DSSC in this study shows excellent stability. The cell with bare PC liquid electrolyte shows instability. Figure 7 shows at-rest stability and

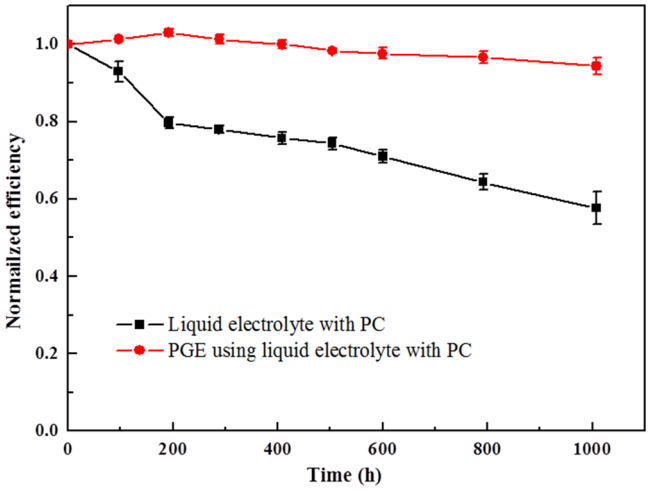

Figure 7. At-rest stability and batch to batch reproducibility data of the DSSC using PGE with PC liquid electrolyte and of the DSSC using bare PC liquid electrolyte (without PGE).

batch-to-batch reproducibility of the DSSC using PGE with 76.7 wt % of the PC liquid electrolyte and also that of the cell with bare PC liquid electrolyte. In this experiment, the cells were sealed, using an UV adhesive as the first layer and a hot molten adhesive as the second layer. The cell efficiencies were measured everyday during the first week to obtain the average value for the first week, and thereafter every weekend; the cell was stored in the dark at room temperature during this test period. Efficiencies were normalized to the average value of the first week, because, according to our experience, the cell efficiency reaches a stable value at room temperature in about 7 days. In spite of the fact that the boiling point of PC is very high, at 242 °C, the overall power conversion efficiency of the DSSC using PGE shows a decrease only by about 5% after 1000 h. On the contrary, the DSSC with the PC liquid electrolyte lost 39% of its initial power conversion efficiency after the same period.

CONCLUSIONS

The POE-PAI polymer gel was observed to absorb conventional liquid electrolytes prepared with different solvents including PC, DMF, and NMP. The morphology of the copolymer after absorbing liquid electrolytes in PC solvent showed a 3D interconnected nanochannels by FE-SEM. The polymer gel was thus used as the matrix for the liquid electrolytes to prepare PGE for QSS-DSSCs. The conductivity of the PGE with PC has increased steeply with the concentration of the redox couple used in the DSSCs and reached a maximum value of 10.9 mS/cm with 0.1 M LiI and 0.05 M I_2. All the DSSCs using the PGE with different liquid electrolytes showed higher photovoltaic performance than their counterparts with bare liquid electrolytes, i.e., without the copolymer. Among the three solvents, PC exhibits the best performance in DSSC because of the highest conductivity and the lowest donor number of PC, compared to those of DMF and NMP. By using the PGE with PC, the DSSC showed a high η of 8.31%, whereas its counterpart with bare PC liquid electrolyte showed an η of only 7.89%. The concentration of the PC liquid electrolyte was optimized to be 76.7 wt % to achieve this photovoltaic performance. Electrochemical impedance spectroscopy parameters are consistent with the photovoltaic parameters of the DSSCs. The IPCE values of the cells with pure PC liquid electrolyte and with the PGE containing 76.7 wt % of the liquid electrolyte agree very well with the corresponding J_{SC} values. The overall power conversion efficiency of the DSSC using PGE with PC liquid electrolyte showed a decrease only by about 5% after 1000 h, while the DSSC with the bare PC liquid electrolyte lost 39% of its initial power conversion efficiency after the same period.

ASSOCIATED CONTENT

Supporting Information

Cross sectional FE-SEM images and incident photo-to-current conversion efficiency (IPCE) curves of the DSSCs. This material is available free of charge via the Internet at http://pubs.acs.org.

AUTHOR INFORMATION

Corresponding Authors

*J.-J. Lin. Tel: +886-2-3366-5312. Fax: +886-2-3366-5237. E-mail: jianglin@ntu.edu.tw.

*K.-C. Ho. Tel: +886-2-2366-0739. Fax: +886-2-2362-3040. E-mail: kcho@ntu.edu.tw.

Notes

The authors declare no competing financial interest.

ACKNOWLEDGMENTS

We acknowledge the financial supports received from the Ministry of Economic Affairs (101-EC-17-A-08-S1-205) and the Ministry of Science and Technology (MOST) of Taiwan.

REFERENCES

(1) Nazeeruddin, M. K.; Angelis, F. D.; Fantacci, S.; Selloni, A.; Viscardi, G.; Liska, P.; Ito, S.; Takeru, B.; Grätzel, M. Combined Experimental and DFT-TDDFT Computational Study of Photoelectrochemical Cell Ruthenium Sensitizers. *J. Am. Chem. Soc.* **2005**, *127*, 16835−16847.

(2) Hagfeldt, A.; Grätzel, M. Molecular Photovoltaics. *Acc. Chem. Res.* **2000**, *33*, 269−277.

(3) Durrant, J. R.; Haque, S. A. Solar Cells: A Solid Compromise. *Nat. Mater.* **2003**, *2*, 362−363.

(4) Han, H. W.; Liu, W.; Zhang, J.; Zhao, X.-Z. A Hybrid Poly(ethylene oxide)/ Poly(vinylidene fluoride)/TiO_2 Nanoparticle Solid-State Redox Electrolyte for Dye-Sensitized Nanocrystalline Solar Cells. *Adv. Funct. Mater.* **2005**, *15*, 1940−1944.

(5) Li, P. J.; Yuan, S. S.; Tang, Q. W.; He, B. L. Robust Conducting Gel Electrolytes for Efficient Quasi-Solid-State Dye-Sensitized Solar Cells. *Electrochim. Acta* **2014**, *137*, 57−64.

(6) Reiter, J.; Vondrak, J.; Michalek, J.; Micka, Z. Ternary Polymer Electrolytes with 1-methylimidazole based Ionic Liquids and Aprotic Solvents. *Electrochim. Acta* **2006**, *52*, 1398−1408.

(7) Zakeeruddin, S. M.; Grätzel, M. Solvent-Free Ionic Liquid Electrolytes for Mesoscopic Dye-Sensitized Solar Cells. *Adv. Funct. Mater.* **2009**, *19*, 2187−2202.

(8) Bach, U.; Lupo, D.; Comte, P.; Moser, J. E.; Weissortel, F.; Salbeck, J.; Spreitzer, H.; Gratzel, M. Solid-State Dye-Sensitized Mesoporous TiO_2 Solar Cells with High Photon-to-Electron Conversion Efficiencies. *Nature* **1998**, *395*, 583−585.

(9) Kumara, G. R. A.; Konno, A.; Shiratsuchi, K.; Tsukahara, J.; Tennakone, K. Dye-Sensitized Solid-State Solar Cells: Use of Crystal Growth Inhibitors for Deposition of the Hole Collector. *Chem. Mater.* **2002**, *14*, 954−955.

(10) Ni, Y.; Jin, Z.; Fu, Y. Electrodeposition of p-Type CuSCN Thin Films by a New Aqueous Electrolyte with Triethanolamine Chelation. *J. Am. Ceram. Soc.* **2007**, *90*, 2966−2973.

(11) Nogueira, A. F.; Longo, C.; De Paoli, M. A. Polymers in Dye Sensitized Solar Cells: Overview and Perspectives. *Coord. Chem. Rev.* **2004**, *248*, 1455−1468.

(12) Freitas, J. N. D.; Nogueira, A. F.; Paoli, M. A. D. New Insights into Dye-Sensitized Solar Cells with Polymer Electrolytes. *J. Mater. Chem.* **2009**, *19*, 5279−5294.

(13) Dong, R. X.; Shen, S. Y.; Chen, H. W.; Wang, C. C.; Shih, P. T.; Liu, C. T.; Vittal, R.; Ho, K. C.; Lin, J. J. A Novel Polymer Gel Electrolyte for Highly Efficient Dye-Sensitized Solar Cells. *J. Mater. Chem. A* **2013**, *1*, 8471−8478.

(14) Agarwala, S.; Peh, C. K. N.; Ho, G. W. Highly Stable Quasi-Solid State Dye Sensitized Solar Cell: Improved Performance Using Diphenylamine in Filler Free KI and LiI Electrolyte. *ACS Appl. Mater. Interfaces* **2011**, *3*, 2383−2391.

(15) Kuang, D.; Wang, P.; Ito, S.; Zakeeruddin, S. M.; Grätzel, M. Stable Mesoscopic Dye-Sensitized Solar Cells Based on Tetracyanoborate Ionic Liquid Electrolyte. *J. Am. Chem. Soc.* **2006**, *128*, 7732−7733.

(16) Mohmeyer, N.; Kuang, D.; Wang, P.; Schmidt, H. W.; Zakeeruddin, S. M.; Grätzel, M. An Efficient Organogelator for Ionic Liquids to Prepare Stable Quasi-Solid-State Dye-Sensitized Solar Cells. *J. Mater. Chem.* **2006**, *16*, 2978−2983.

(17) Wu, J.; Lan, Z.; Lin, J.; Huang, M.; Hao, S.; Sato, T.; Yin, S. A Novel Thermosetting Gel Electrolyte for Stable Quasi-Solid-State Dye-Sensitized Solar Cells. *Adv. Mater.* **2007**, *19*, 4006−4011.

(18) Chen, C. L.; Teng, H.; Lee, Y. L. In Situ Gelation of Electrolytes for Highly Efficient Gel-State Dye-Sensitized Solar Cells. *Adv. Mater.* **2011**, *23*, 4199−4204.

(19) Cao, F.; Oskam, G.; Searson, P. C. A Solid State, Dye Sensitized Photoelectrochemical Cell. *J. Phys. Chem.* **1995**, *99*, 17071−17073.

(20) Tu, C. W.; Liu, K. Y.; Chien, A. T.; Lee, C. H.; Ho, K. C.; Lin, K. F. Performance of Gelled-Type Dye-Sensitized Solar Cells Associated with Glass Transition Temperature of the Gelatinizing Polymers. *Eur. Polym. J.* **2008**, *44*, 608−614.

(21) Wang, P.; Zakeeruddin, S. M.; Moser, J. E.; Nazeeruddin, M. K.; Sekiguchi, T.; Grätzel, M. A Stable Quasi-Solid-State Dye-Sensitized Solar Cell with an Amphiphilic Ruthenium Sensitizer and Polymer Gel Electrolyte. *Nat. Mater.* **2003**, *2*, 402−407.

(22) Yang, H.; Huang, M.; Wu, J.; Lan, Z.; Hao, S.; Lin, J. The Polymer Gel Electrolyte Based on Poly(methyl methacrylate) and Its Application in Quasi-Solid-State Dye-Sensitized Solar Cells. *Mater. Chem. Phys.* **2008**, *110*, 38−42.

(23) Patela, R.; Seoa, J. A.; Koha, J. H.; Kima, J. H.; Kangb, Y. S. Dye-Sensitized Solar Cells Employing Amphiphilic Poly(ethylene glycol) Electrolytes. *J. Photochem. Photobiol., A* **2011**, *217*, 169−176.

(24) Wu, J.; Hao, S.; Lan, Z.; Lin, J.; Huang, M.; Huang, Y.; Fang, L.; Yin, S.; Sato, T. A Thermoplastic Gel Electrolyte for Stable Quasi-Solid-State Dye-Sensitized Solar Cells. *Adv. Funct. Mater.* **2007**, *17*, 2645−2652.
(25) Wang, P.; Zakeeruddin, S. M.; Exnar, I.; Grätzel, M. High Efficiency Dye-Sensitized Nanocrystalline Solar Cells Based on Ionic Liquid Polymer Gel Electrolyte. *Chem. Commun.* **2002**, *24*, 2972−2973.
(26) Benedetti, J. E.; Goncalves, A. D.; Formiga, A. L. B.; Paoli, M. A.; Li, X.; Durrant, J. R.; Nogueira, A. F. A Polymer Gel Electrolyte Composed of a Poly(ethylene oxide) Copolymer and the Influence of Its Composition on the Dynamics and Performance of Dye-Sensitized Solar Cells. *J. Power Sources* **2010**, *195*, 1246−1255.
(27) Yu, Q. J.; Yu, C. L.; Guo, F. Y.; Wang, J. Z.; Jiao, S. J.; Gao, S. Y.; Li, H. T.; Zhao, L. C. A Stable and Efficient Quasi-Solid-State Dye-Sensitized Solar Cell with a Low Molecular Weight Organic Gelator. *Energy Environ. Sci.* **2012**, *5*, 6151−6155.
(28) Kebede, Z.; Lindquist, S. E. Donor−Acceptor Interaction between Non-Aqueous Solvents and I_2 to Generate I_3^-, and Its Implication in Dye Sensitized Solar Cells. *Sol. Energy Mater. Sol. Cells* **1999**, *57*, 259−275.
(29) Cahen, D.; Hodes, G.; Gratzel, M.; Guillemoles, J. F.; Riess, I. Nature of Photovoltaic Action in Dye-Sensitized Solar Cells. *J. Phys. Chem. B* **2000**, *104*, 2053−2059.
(30) Kang, T. S.; Chun, K. H.; Hong, J. S.; Moon, S. H.; Kim, K. J. Enhanced Stability of Photocurrent-Voltage Curves in Ru(II)-Dye-Sensitized Nanocrystalline TiO_2 Electrodes with Carboxylic Acids. *J. Electrochem. Soc.* **2000**, *147*, 3049−3053.
(31) Lee, K. M.; Suryanarayanan, V.; Ho, K. C. Influences of Different TiO_2 Morphologies and Solvents on the Photovoltaic Performance of Dye-Sensitized Solar Cells. *J. Power Sources* **2009**, *188*, 635−641.